Crystal Engineering Involving C−H···N Weak Hydrogen Bonds: A Diquinoxaline Lattice Inclusion Host with a Preference for Polychlorocarbon Guests

Christopher E. Marjo,[a] Roger Bishop,*[a] Donald C. Craig,[a] and Marcia L. Scudder[a]

Keywords: Crystal engineering / Inclusion compounds / Nitrogen heterocycles / Hydrogen bonds / Crystal structures

The di(1,8-naphthryridine) **7** and diquinoxaline **12** derivatives were synthesised as potential new lattice inclusion hosts where strong hydrogen bonding interactions would be absent. A number of potential supramolecular synthons (such as aryl face-face, aryl edge-face, halogen-halogen, C–H···N, nitrogen-halogen) were expected to be accessible, with competing combinations of these weak attractions providing the best (but probably different) type of host-guest structure in each case. While the former compound turned out to be unstable, the latter proved to be a versatile host which preferred to trap small polychloroalkane guests. The X-ray structures of **12**·(chloroform)$_2$, (**12**)$_2$·(tetrahydrofuran), and (**12**)$_2$·(1,1,2,2-tetrachloroethane) are reported and shown to have different lattice packing where the guests occupy layers, parallel tubes, and molecular boxes, respectively. The detailed interplay of the above synthons in forming these structures is described in crystal engineering terms. Most significantly, the C–H···N weak hydrogen bond plays a major role in all three inclusion structures. Both single linear and double cyclic interactions are involved in molecular edge-edge assembly of the host **12**. Several new types of double cyclic interactions were discovered revealing that the C–H···N interaction is a key synthon for crystal engineering involving nitrogen heteroaromatic compounds.

Introduction

The majority of inclusion compounds result from interaction of a pre-formed host receptor molecule with a guest species. Lattice inclusion (or clathrate) compounds, on the other hand, arise through multiple interactions of the hosts and guests constituting a crystal lattice[1,2] and consequently the design of new examples represents a significant synthetic challenge.[3] One approach is to use crystal engineering which seeks to discover, understand, and ultimately control, the specific types of intermolecular forces determining lattice packing arrangements.[4] Robust interactions may be regarded as supramolecular synthons which can be used reliably towards the synthesis of new molecular assemblies.[5] To date, hydroxy group hydrogen bonding ···H−O···H−O···H−O··· has been the commonest means of construction employed towards the design of new clathrating hosts.[1,2] The method employed in this current work is significantly different. It relies instead on intermolecular competition between a number of weaker attractions, the best combination of which will lead to the observed clathrate compound. The C−H···N weak hydrogen bond is a crucial synthon in this synthetic approach.

The C−H···N interaction[6] is generally regarded as being an archetype of the weak hydrogen bond.[7] However, while histograms of X-ray intermolecular contacts (frequency versus interatomic distance) compiled by Rowland and Taylor[8] revealed a maximum for the weak hydrogen bond C−*H*···*O* at just under 3 Å, no analogous peak was apparent for C−*H*···*N*. This could mean that the C−H···N motif forms less often than C−H···O,[9] or merely that insufficient appropriate structures have been reported so far. Whatever the explanation, there is no question that the application of the C−H···N synthon in crystal engineering has been limited and that currently it is a poor cousin relative to C−H···O.[7] In this paper we report on ways that the C−H···N synthon can contribute to making new lattice inclusion compounds.

Earlier we described the solid state interactions present between molecules of the racemic diquinoline derivative **1**.[10] Amongst these was a new intermolecular motif, the edge-edge aryl C−H···N dimer (*C*−H···*N* 3.55 Å, Figure 1a), which has also been noted by other workers in alternative systems.[11] Since edge-edge assembly is not normally encountered between aromatic hydrocarbons (where face-face and edge-face contacts predominate) this centrosymmetric dimer provides an important packing mode for many aromatic nitrogen compounds.[10]

Conversion of **1** into the *exo,exo*-dibromide **2** created a potent host molecule with a strong preference for including small polyhalogenated guests (Scheme 1).[12] The aryl C−H···N dimer motif is retained in solid **2**·$CHCl_3$ (Figure 1b) where one host **2** nitrogen atom participates in a centrosymmetric dimer (*C*−H···*N* 3.65 Å) while the second forms a hydrogen bond to the chloroform guest (*C*−H···*N* 3.37 Å). Our preliminary results[10,12] therefore indicate that the centrosymmetric aryl C−H···N dimer is an important synthon for pairing opposite enantiomers in the solid state. Here we explore its role in the potential heteroaromatic

[a] School of Chemistry, The University of New South Wales, UNSW Sydney, NSW 2052, Australia
Fax: (internat.) +61-2/9385-6141
E-mail: r.bishop@unsw.edu.au

Supporting information for this article is available on the WWW under http://www.wiley-vch.de/home/eurjoc or from the author.

  1434−193X/01/0305−0863 $ 17.50+.50/0

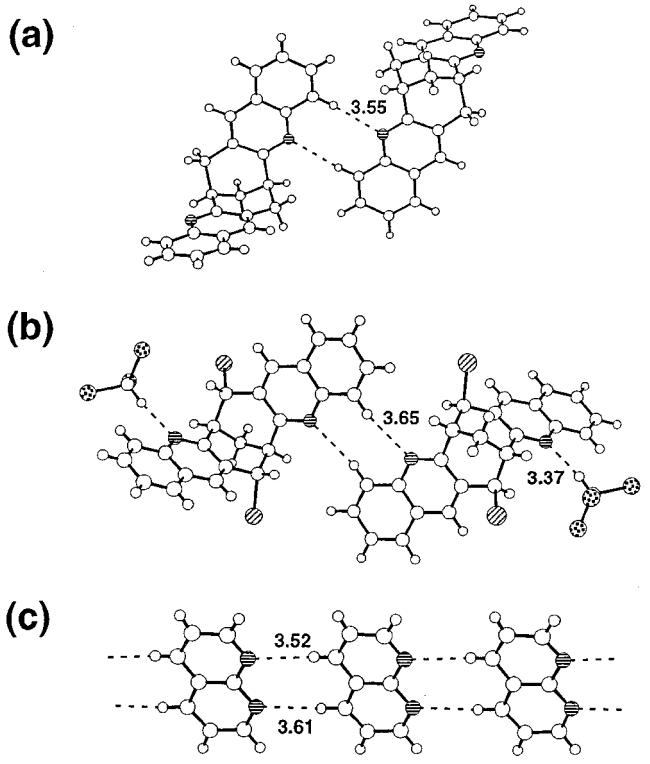

Figure 1. (a) The centrosymmetric edge-edge aryl C−H···N dimer interaction (C−H···N 3.55 Å) present between opposite enantiomers of solid **1**; (b) centrosymmetric arrangement of the C−H···N weak hydrogen bonds, aryl *C*−H···*N* 3.65 Å and Cl_3C−H···*N* 3.37 Å, present in solid **2**·($CHCl_3$); (c) the asymmetric C−H···N dimer (*C*−H···*N* 3.52 and 3.61 Å) present in solid 1,8-naphthyridine **3**; all weak hydrogen bonds are indicated by dashed lines; atom designators used here and in subsequent figures: N horizontal hatching, Br diagonal hatching, and Cl heavy stippling

hosts **7** and **12** which contain four, rather than two, nitrogen atoms.

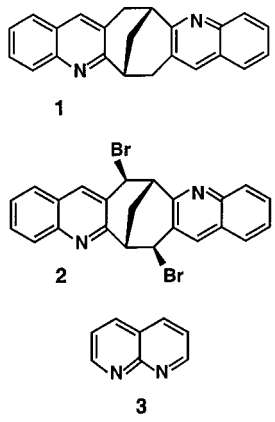

Scheme 1. Structures of heteroaromatic compounds **1**−**3** whose crystal structures involve dimeric C−H···N weak hydrogen bonds

Results and Discussion

Di(1,8-naphthryridine) Derivative 7

Crystalline 1,8-naphthyridine[13] **3** also contains dimeric edge-edge aryl C−H···N interactions, but this different motif involves two dissimilar *C*−H···*N* distances (3.52 and 3.61 Å from room temperature X-ray studies). This has been confirmed at 163 K where values of 3.48 and 3.57 Å were recorded. Hence, the aryl C−H···N dimers are asymmetric and participation of both edges of the **3** molecules results in formation of infinite, slightly stepped, chains as illustrated in Figure 1c.

This observation suggested that other varieties of aryl C−H···N dimer could well be involved in the edge-edge assembly of new lattice inclusion hosts. The *exo*,*exo*-dibromo di(1,8-naphthyridine) **(7)** was therefore an attractive target for investigation and was synthesised as shown in Scheme 2. Friedländer condensation[14] of 2-aminonicotinaldehyde **(4)**[15] and bicyclo[3.3.1]nonane-2,6-dione **(5)**[16] afforded the di(1,8-naphthyridine) **6** in modest yield, with free radical bromination using *N*-bromosuccinimide (NBS) completing the preparation.

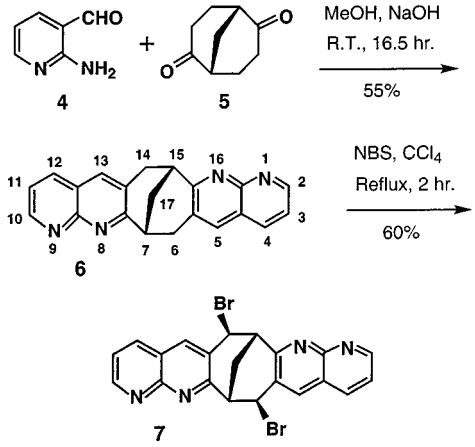

Scheme 2. Preparation of the dibromo di(1,8-naphthyridine) derivative **7**

All spectral data recorded were in full agreement with the proposed structure **7**, but this new compound proved to be unstable in solution and attempts to obtain crystals from chloroform or 1,1,1-trichloroethane resulted in intractable gums. This behaviour may be attributable to the less hindered and more reactive N1/N9 lone pairs (compared to N8/N16) reacting with the benzylic C6/C14 brominated sites of **7**. In support of this possibility, **6** was found to react with benzyl bromide giving the hygroscopic double salt **8** in very high yield while the diquinoline derivative **1** was completely unreactive under identical conditions (Scheme 3).

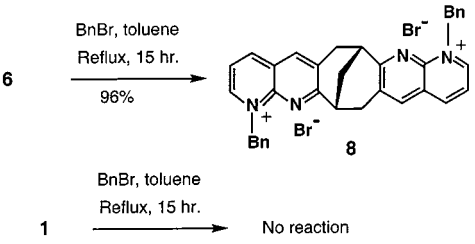

Scheme 3. Comparison of the reactivity of the diquinoline **1** and di(1,8-naphthyridine) **6** compounds with benzyl bromide

A search of the Cambridge Structural Database (CSD)[17] for dimeric interactions analogous to that observed in solid

3, specifying *C*−H···*N* distances under 3.70 Å with equal or dissimilar lengths, failed to reveal any further examples.

Diquinoxaline Analogue 12

Our attention therefore turned to the *exo*,*exo*-dibromo diquinoxaline derivative **12** whose synthesis employed a heterocyclic analogue of the Friedländer reaction.[18] Thus, the double condensation of benzofurazan *N*-oxide **(9)**[19] with dione **5** gave the *N*-oxide **10** which was reduced in high yield by sodium dithionite to yield the diquinoxaline derivative **11**. Finally, benzylic bromination using NBS afforded the target compound **12** as outlined in Scheme 4.

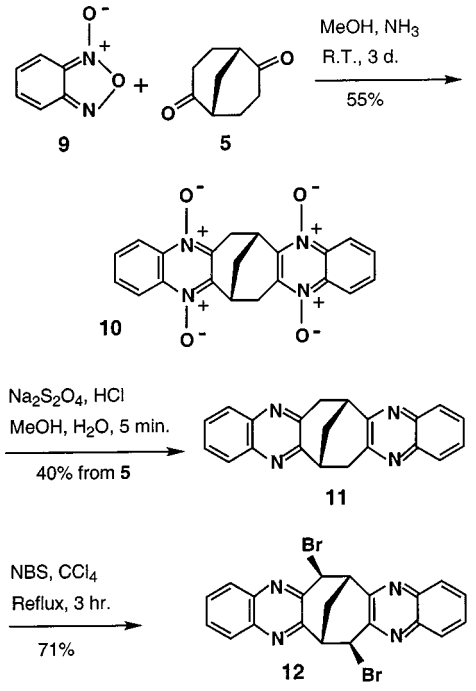

Scheme 4. Synthesis of the dibromo diquinoxaline inclusion host **12**

The dibromo diquinoxaline **12** proved to be an excellent host molecule, forming inclusion compounds on crystallisation from chloroform, 1,1,1-trichloroethane, 1,1,2-trichloroethane, 1,1,2,2-tetrachloroethane, tetrahydrofuran (THF) and benzene. Apart from the chloroform compound (host:guest stoichiometry of 1:2), solution ^{1}H NMR spectroscopy indicated that all of these were 2:1 compounds. Potential guests which were not trapped under our conditions were dichloromethane, bromoform, 1,2-dibromoethane, 1,2,3-trichloropropane, dioxane, ethyl acetate, and cyclohexane. Like compound **2**, the dibromo compound **12** shows a preference for inclusion of polyhalocarbon guests, though this selectivity was not as pronounced. Whereas **2** tended to produce crystalline inclusion compounds with one-carbon polyhalo guests,[12] the new host **12** favoured two-carbon polychlorocarbons. The single crystal X-ray structures of the chloroform, tetrahydrofuran, and 1,1,2,2-tetrachloroethane inclusion compounds were determined and found to adopt different lattice packing and symmetry. Table 1 lists numerical details of the solution and refinement of these structures.

Crystal Structure of 12·$(CHCl_3)_2$

The 1:2 inclusion compound of **12** with chloroform showed quite different stoichiometry, lattice packing and symmetry compared to the earlier compound **2**·$CHCl_3$, despite the common guest and both hosts having almost identical shapes and volumes. These calculated molecular volumes are V_o = 338 Å^3 for **2**, and V_o = 328 Å^3 for **12** (see Experimental Section). The space groups adopted by the two inclusion compounds are $P2_1/c$ and $C2/c$, respectively.

In the crystalline state, molecules tend to be arranged to maximise use of space and minimise intermolecular repulsions. Hence molecular crystals usually occupy 60−80% of the available volume.[20] Smaller values are often associated with amorphous substances, but lattice inclusion can provide means for a poorly packed host to increase its occupancy above 60%.[21] If **12** were to trap chloroform in the same host lattice as **2**·$CHCl_3$ then the calculated occupancy would be 69%. Since the observed occupancy in **12**·$(CHCl_3)_2$ is only marginally higher (70%), this difference in inclusion behaviour is difficult to explain if only close-packing arguments are invoked.

In structure **12**·$(CHCl_3)_2$ adjacent host molecules of opposite chirality are linked by aryl C−H···N dimers, but these differ in several respects from those observed previously.[10] First, the dimer joining two diquinolines in **2**·$CHCl_3$.forms on the opposite side (*anti*-) of the central bicyclo[3.3.1]nonane ring to the bromine substituent, while in **12**·$(CHCl_3)_2$ it is situated on the same side (*syn*-) (see Figure 2). While the molecular structure of **2** precludes a *syn*-interaction, in principle **12** could have interacted in either sense.

Next, the *C*−H···*N* distance in **12**·$(CHCl_3)_2$ increases significantly to 3.88 Å, presumably because of greater congestion in the *syn*-interaction mode. Table 2 lists this, and all subsequent, data on the C−H···N interactions encountered during this work. Thirdly, each host molecule subtends two identical dimers which results in assembly of these molecules into infinite chains with corrugated surfaces (Figure 3). Despite these differences, the aryl C−H···N dimers in structure **12**·$(CHCl_3)_2$ are still centrosymmetric, as found for 53 of the 54 cases recorded in our earlier survey.[10]

Figure 4 shows the unit cell diagram (viewed down *b*) where these infinite chains can be seen running along the short *ac* diagonal. The packing of **12** can also be described in terms of layers in the *bc* plane, with these layers being cross-linked diagonally by the C−H···N dimers. Within each layer of **12** there are two different aryl face-face interaction types (Figure S1, Supporting Information). The V-shaped host molecules can be considered as having concave (*endo*-) and convex (*exo*-) surfaces. The unbroken arrows indicate weakly overlapping benzo face-face interactions where the concave surfaces come together, and the broken arrows show strongly overlapping heteroaryl face-face interactions where the convex surfaces abut. Their respective interplanar distances are approximately 3.4 and 3.7 Å.

Table 1. Numerical details of the solution and refinement of the structures of the three inclusion compounds

Compound	**12** and chloroform	**12** and tetrahydrofuran	**12** and 1,1,2,2-tetrachloroethane
Formula	$C_{21}H_{14}Br_2N_4{\cdot}(CHCl_3)_2$	$(C_{21}H_{14}Br_2N_4)_2{\cdot}C_4H_8O$	$(C_{21}H_{14}Br_2N_4)_2{\cdot}C_2H_2Cl_4$
Formula mass	720.9	1036.5	1132.2
Crystal description	– [a]	{110}(00−1)(102)(-102)	{110}{001}
Space group	*C*2/*c*	$P2_12_12_1$	*Pbcn*
a [Å]	17.897(6)	11.670(1)	11.663(2)
b [Å]	10.627(2)	13.170(1)	13.195(3)
c [Å]	16.334(6)	27.649(2)	27.444(5)
β [°]	120.81(1)	(90)	(90)
V [Å^3]	2668(1)	4249.2(6)	4223(2)
T [°C]	21(1)	21(1)	21(1)
Z	4	4	4
$D_{calcd.}$ [g cm^{-3}]	1.79	1.62	1.78
Radiation, λ [Å]	Mo-K_α, 0.7107	Cu-K$_\alpha$, 1.5418	Cu-K$_\alpha$, 1.5418
μ [cm^{-1}]	36.4	50.3	74.51
Crystal dimensions [mm]	–[a]	0.27 × 0.27 × 0.08	0.18 × 0.18 × 0.19
Scan mode	$\theta/2\theta$	$\theta/2\theta$	$\theta/2\theta$
$2\theta_{max.}$ [°]	50	140	140
ω scan angle	0.50 + 0.35tan θ	0.50 + 0.15tan θ	0.60 + 0.15tan θ
No. of intensity measurements	2354	4489	4508
Criterion for observed reflection	$I/\sigma(I) > 3$	$I/\sigma(I) > 3$	$I/\sigma(I) > 3$
No. of indep. obsd. reflections	1562	3492	2117
No. of reflections (*m*) and	1562	3492	2117
Variables (*n*) in final refinement	153	234	271
$R = \Sigma^m\|\Delta F\|/\Sigma^m\|F_o$	0.049	0.045	0.041
$R_w = [\Sigma^m w\|\Delta F\|^2/\Sigma^m w\|F_o\|^2]^{1/2}$	0.060	0.064	0.048
$s = [\Sigma^m w\|\Delta F\|^2/(m - n)]^{1/2}$	1.97	2.08	1.47
Crystal decay	1 to 0.94	None	1 to 0.98
Max., min. transmission coefficients	– [a]	0.67, 0.20	0.36, 0.27
R for (no. of) multiple measurements	0.058 (132)	–	–
Largest peak in final diff. map/ e Å^{-3}	1.06	0.96	0.55

[a] This crystal was sealed in a tube therefore making it impossible determine its crystal faces or to apply absorption corrections.

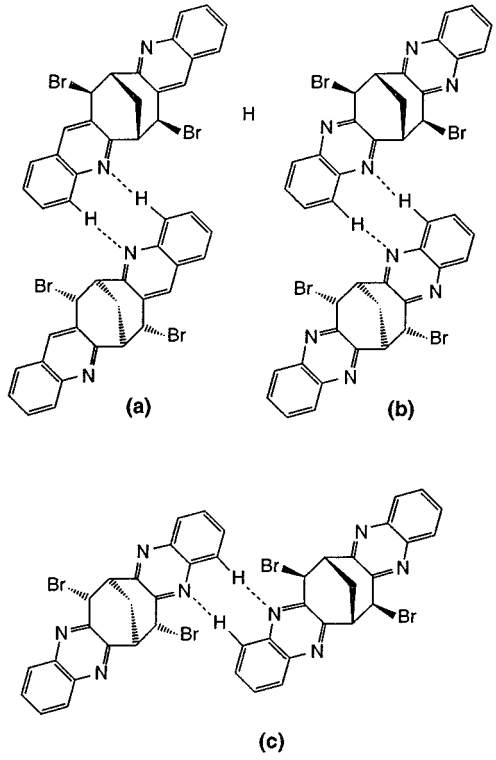

Figure 2. (a) The dimeric C−H···N interaction in **2**·($CHCl_3$) where it must be positioned *anti* to the bromine atom on the same edge of the diquinoline **2**; (b) The hypothetical *anti* arrangement which could, in principle, be formed between molecules of the diquinoxaline host **12**; (c) the alternative *syn*-arrangement which is actually adopted in solid **12**·($CHCl_3$)$_2$

This arrangement only occupies some 49% of the crystal volume and leaves void spaces in the form of corrugated channels in the *bc* plane between the layers. These channels are occupied by the chloroform guest molecules as shown in Figure 4. The 2:1 host:guest stoichiometry increases the molecular volume to 70%. In contrast to structure **2**·$CHCl_3$, the hosts and guests are not hydrogen bonded together. Instead they are associated through N···Cl interactions which involve the two remaining nitrogen atoms not already forming aryl C−H···N dimers. Each nitrogen interacts with two guests, and each guest with two nitrogens, through N···Cl interactions of 3.04 and 3.30 Å (with N···Cl−C angles of 167 and 156°, respectively). These N···Cl interactions help organise the interlayer $CHCl_3$ guests into spiral arrangements along the *b* direction (Figure S2, Supporting Information).

Interactions between nitrogen and haloalkanes are common in molecular crystals and are generally regarded as being of charge transfer nature.[22] The N···Cl distances are typically 3.00−3.45 Å.[23] When the nitrogen atom is present in an aromatic ring the N···Cl−C angle tends to be around 180° depending on distortions induced by crystal packing. A computational study has estimated the energy of association for N···Cl at around 5 kJ mol^{-1}.[24]

The host *exo*-bromine atoms protrude into the channels leading to multiple interhalogen attractions which provide significant stabilisation of the co-crystals. There is a host-host Br···Br interaction (3.86 Å) which further cross-links the host layers, and also a guest-guest Cl···Cl interaction of

Table 2. Characteristics of intermolecular C−H···N weak hydrogen bonds from crystallographic determinations.

Compound	$C_{\circ}$−H···*N* (Å)	$C_{\circ}$−*H*···*N* (Å)	Interaction type	Angle (°)	Type of interaction	Comments
1	3.55	2.56	Ar−H···N	84.2[a]	Centrosymmetric dimer	ref. [10]
2·$CHCl_3$	3.65	2.67	Ar−H···N	89.0 [a]	Centrosymmetric dimer	ref. [12]
	3.37	2.40	Cl_3C−H···N	163[b]	Guest-host interaction	ref. [12]
3	3.52	2.73[c]	Ar−H···N	66.9 [a]	Asymmetric dimer	Structure at ambient T, Refcode NAPTYR, ref. [13a]
	3.61	2.81[d]	Ar−H···N	66.0 [a]	Asymmetric dimer	
3	3.48	2.61	Ar−H···N	67.1 [a]	Asymmetric dimer	Structure at 163 K, Refcode NAPTYR11, ref. [13b]
	3.57	2.75	Ar−H···N	66.2 [a]	Asymmetric dimer	
12·$(CHCl_3)_2$	3.88	2.91	Ar−H···N	82.4 [a]	Centrosymmetric dimer	
$(\mathbf{12})_2$·C_4H_8O	3.59	2.67	Ar−H···N	68.2 [a]	Asymmetric dimer no. 1	
	3.49	2.59	BrC−H···N	149 [b]	Asymmetric dimer no. 1	
	3.50	2.59	Ar−H···N	70.6 [a]	Asymmetric dimer no. 2	
	3.41	2.54	BrC−H···N	145 [b]	Asymmetric dimer no. 2	
	3.62	2.72	C−H···N	149 [b]	Single interaction	Wall-wing interaction no. 1
	3.91	3.03	Ar−H···N	147 [b]	Single interaction	Wall-wing interaction no. 1
	3.65	2.74	C−H···N	151 [b]	Single interaction	Wall-wing interaction no. 2
	3.90	3.03	Ar−H···N	147 [b]	Single interaction	Wall-wing interaction no. 2
$(\mathbf{12})_2$·$C_2H_2Cl_4$	3.79	3.00	Ar−H···N	57.9 [a]	Asymmetric dimer	
	3.59	2.72	BrC−H···N	146 [b]	Asymmetric dimer	
	3.64	2.73	C−H···N	151 [b]	Single interaction	Wall-wing interaction
	4.00	3.16	Ar−H···N	142 [b]	Single interaction	Wall-wing interaction

[a] Angle is that between the C···N vector of the intermolecular contact and the normal to the plane of the aryl ring containing this carbon atom. A value of 90° would indicate a perfectly planar array. − [b] C−H···N angle. − [c] Hydrogen position from published structure. − [d] Calculated hydrogen position used.

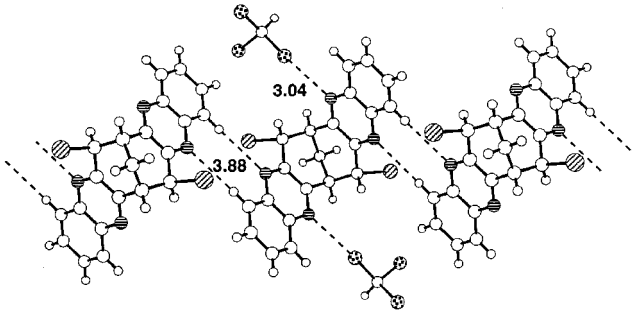

Figure 3. The centrosymmetric arrangement of double aryl *C*−H···*N* (3.88 Å) weak hydrogen bonds and single HCl_2C−*Cl*···*N* (3.04 Å) interactions present in **12**·$(CHCl_3)_2$ where both interaction types are indicated by dashed lines; the resulting chains of **12** molecules run along the *ac* diagonal

3.59 Å. In addition, each *exo*-bromine participates in four different host-guest Br···Cl interactions. The net outcome is a centrosymmetric network of halogen interactions (Figure S3, Supporting Information).

The interhalogen interaction (Cl < Br < I) is well-known as an important supramolecular synthon in solid state chemistry.[4,25] It is noteworthy that here host and guest participate in the less commonly encountered Br···Cl interaction. Interactions between dissimilar halogens can sometimes be stronger than those between like.[26] Intermolecular Cl···Cl distances in crystals are typically around 3.6−3.8 Å, slightly more than twice the van der Waals radius of 1.75 Å for Cl.[27] Since the sum of van der Waals radii for Cl and Br is 3.60 Å, none of the individual halogen-halogen interactions present in **12**·$(CHCl_3)_2$ is especially strong. However, it is the generation of a *network* of interactions which is significant in favouring the **12**−polyhalocarbon combination.

Crystal Structure of $(\mathbf{12})_2$·C_4H_8O

Crystallisation of dibromide **12** from tetrahydrofuran (THF) results in formation of the inclusion compound $(\mathbf{12})_2$·C_4H_8O whose crystals occupy the chiral space group $P2_12_12_1$. Hence the bulk crystalline sample is a conglomerate comprising a 1:1 mixture of pure (+)- and pure (−)-crystals.[28] This chirality does not result, however, from self-resolution of the racemic host enantiomers. Both enantiomers of **12** are present in the asymmetric unit of each crystal.

Once again double C−H···N interactions allow edge-edge packing of the host, but their arrangement is structurally unlike any of the previously observed examples. Although the edge-edge interaction still joins opposite enantiomer it is no longer centrosymmetric and two different types of C−H···N interaction operate from each edge. Furthermore, two dimers of different geometry are subtended from the opposite edges of each molecule of **12** (Figure 5). It is this asymmetry which generates the lattice chirality causing conglomerate formation.

These new C−H···N dimers comprise aryl *C*−H···*N* (3.50 and 3.59 Å) and aliphatic Br*C*−H···*N* (3.41 and 3.49 Å) interactions; the latter being analogous to the Cl_3C−H···*N* hydrogen bond (3.37 Å) present in **2**·$CHCl_3$ (Figure 1b). The dimeric links once again give rise to infinite chains of **12** molecules but only one wing of each V-shaped host molecule interacts in the edge-to-edge fashion forming a molecular wall along *b* (Figure 5). The second wings of the alternating enantiomers are subtended left-right-left-right etc. along the top of the wall, and therefore when viewed along the wall itself these chains have a T-shaped projection when viewed along *b*.

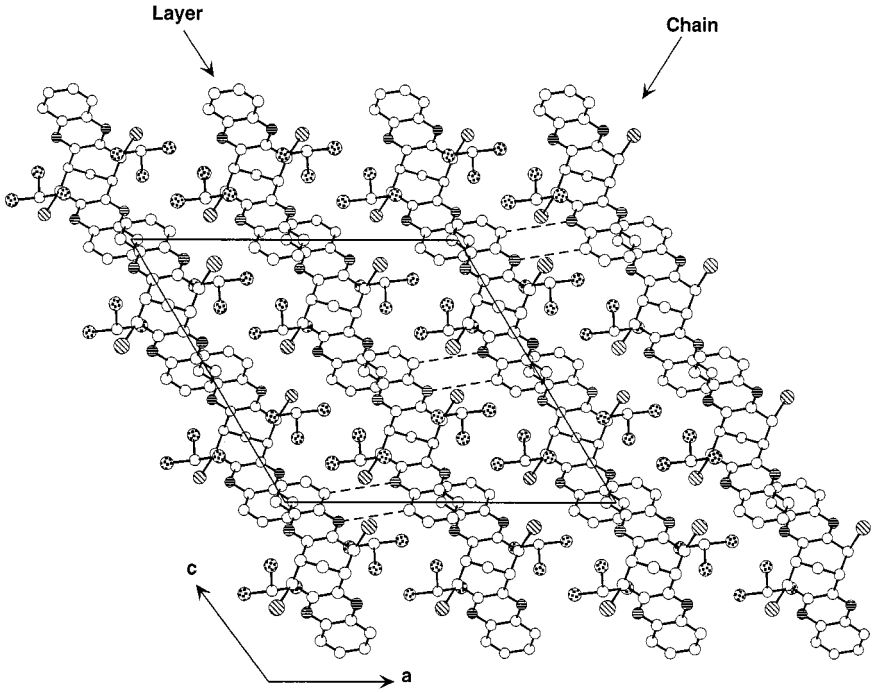

Figure 4. The unit cell of **12**·$(CHCl_3)_2$ with all hydrogen atoms omitted for clarity; hydrogen bonded chains of **12** and their associated guest molecules (see Figure 3) lie along the *ac* diagonal; aryl face-face interactions between **12** molecules in adjacent chains (see Figure S1, Supporting Information) create parallel layers in the *bc* plane; host-host Br···Br, host-guest Br···Cl, and guest-guest Cl···Cl interactions (see Figures S2 and S3, Supporting Information) provide a complex inter-layer network of halogen-halogen attractions which further stabilise the molecular combination in solid **12**·$(CHCl_3)_2$

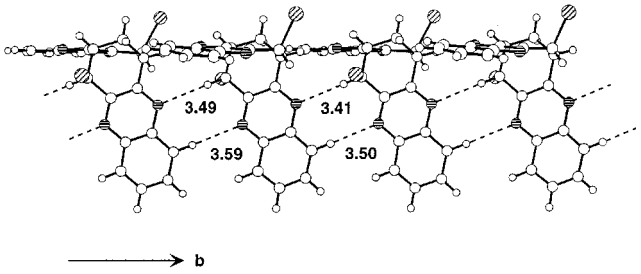

Figure 5. Part of an infinite chain of alternating enantiomers of diquinoxaline **12** molecules in solid (**12**)$_2$·(THF); edge-edge assembly of the host molecules produces a molecular wall along *b* through two dimeric C−H···N motifs of different geometries; these involve aryl *C*−H···*N* hydrogen bonds (3.50 and 3.59 Å) and Br*C*−H···*N* hydrogen bonds (3.41 and 3.49 Å); the second wings of the V-shaped **12** molecules are oriented in-out-in-out along the top of the diagram, producing a chain with a T-shaped cross-section when viewed end-on

Projection in the *ac* plane (Figure 6) shows that the structure is composed of a series of double layers. The T-shaped molecular walls forming the top and bottom of each double layer are directed inwards and interleave with each other. Where the walls are close they participate in aryl face-face overlap (3.6 Å) and where they are distant a THF guest is interposed. These double layers stack on top of each other in the sense -a-b-a-b-, stabilised by two familiar types of intermolecular interaction already discussed for **12**·$(CHCl_3)_2$. The first is an aryl face-face attraction (3.7 Å) and the second is an array of weak Br···Br attractions of 3.71, 3.75 and 3.87 Å.

The top and bottom outer faces of each double layer comprise the alternately subtended wings and, where wings

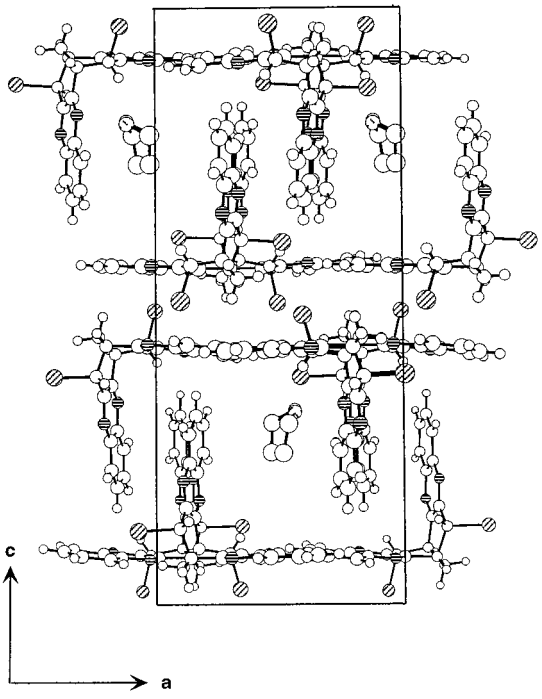

Figure 6. Two double layers, each formed from interleaved T-projection molecular walls, stacked on top of each other involving aryl face-face interactions and Br···Br attractions; within each double layer the up- and down-oriented molecular walls interact through aryl face-face attractions, and the THF guest molecules occupy the tubes formed between these paired walls in (**12**)$_2$·(THF); only one position has been shown for the disordered guest

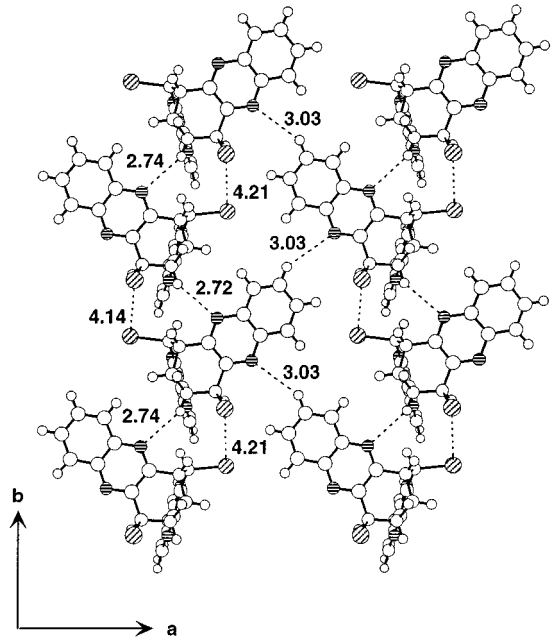

Figure 7. Part of the top surface of a double layer in $(\mathbf{12})_2$·(THF) (see Figure 6) showing how two down-orientated molecular walls of T-shaped cross-section abut; Br···Br (4.14 and 4.21 Å) and aliphatic C−*H*···*N* (2.72 and 2.74 Å) attractions stabilise the top of each T-shaped cross-section wall, while aryl C−*H*···*N* (3.03 Å) weak hydrogen bonds encourage edge-edge assembly of the two T-structures

of neighbouring T cross-sectioned chains abut, they assemble edge to edge as shown in Figure 7. These planar contacts involve two slightly different single aryl Ar-H···N interactions (both 3.03 Å) which are repeated infinitely between the wings of adjacent chains. This arrangement is further stabilised through intermolecular Br···Br (4.14 and 4.21 Å) and C−*H*···*N* contacts (2.72 and 2.74 Å) within the wings themselves. The latter weak hydrogen bonds involve the sp^3 bridgehead hydrogen of the host.

Figure 7 shows a projection view in the *ab* plane of part of the top surface of a double layer in $(\mathbf{12})_2$·C_4H_8O showing two adjacent down-oriented molecular walls This reveals that the molecular walls are sinusoidal in shape. Those subtended downwards from the top, and also those subtended upwards from the bottom, of each double layer run parallel throughout the lattice. In other words the walls orientations remain in phase with each other and the two inter-wall distances (one large, one small) remain constant (Figure 8). Slightly kinked, unobstructed tubes are produced in which the THF guest molecules reside. Hence $(\mathbf{12})_2$·C_4H_8O has a tubulate inclusion topology.

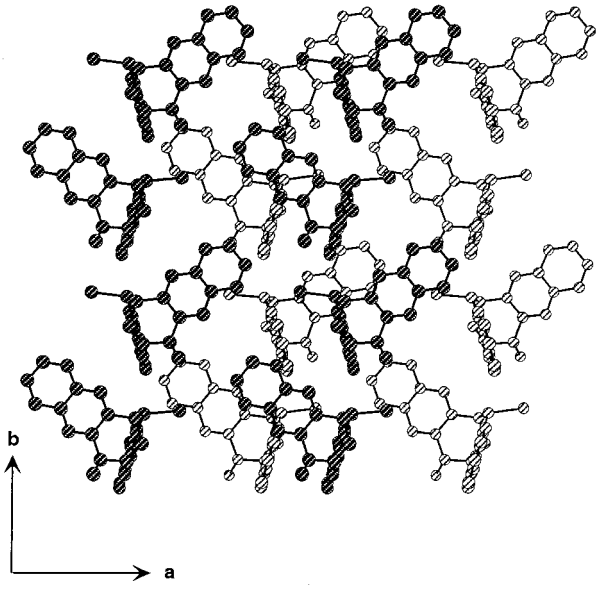

Figure 8. Projection view in the *ab* plane of a double layer in $(\mathbf{12})_2$·(THF), showing a pair of down-orientated molecular walls forming its upper surface (dark hatching) superimposed on a pair of up-oriented molecular walls forming its lower surface (light hatching); the inter-wall distances remain constant along *b* creating parallel sinusoidal tubes which include the THF guests (omitted here for clarity) as a tubulate inclusion compound

From the X-ray data it was not easy to distinguish between guest methylenes and oxygens, therefore an arbitrary assignment has been made in Figure 9 which illustrates just one tube. Guests are also disordered and can occupy two alternative positions in a tube, the one illustrated and an alternative where the THF molecules are located in the positions between the guests in the first. The empty host lattice occupies 62% of the crystal volume and inclusion of the guests raises this to 69%.

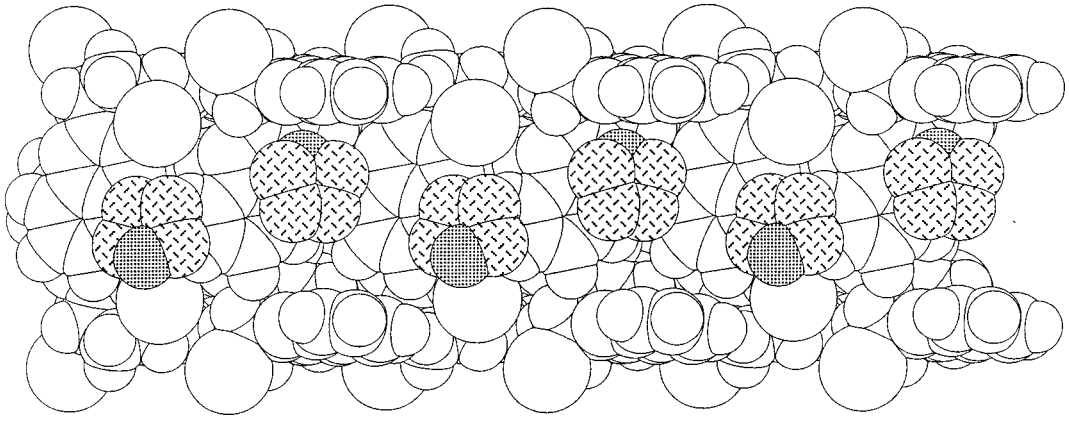

Figure 9. Cut-away view of one sinusoidal tube (along *b*) in $(\mathbf{12})_2$·(THF) showing a typical arrangement of the disordered THF molecules; guest hydrogens are omitted for clarity, carbons are cross-hatched, and oxygens heavily stippled

Crystal Structure of $(12)_2{\cdot}C_2H_2Cl_4$

In the 1,1,2,2-tetrachloroethane inclusion compound the host molecules assemble to produce an extraordinary three-dimensional array of molecular boxes each of which encloses one guest molecule. The unit cell dimensions of this compound are virtually identical to those of $(12)_2{\cdot}C_4H_8O$ and in many respects its structure is its simpler achiral relative.

Once again asymmetric dimeric edge-edge interactions link opposite enantiomers to create a molecular wall along *b*, but this time the interactions subtended by each edge of the wing of **12** are identical. The different C−H···N interactions comprising each dimer are an aryl *C*−H···*N* (3.79 Å) and an aliphatic Br*C*−H···*N* (3.59 Å) (Figure S4, Supporting Information; cf. Figure 5).

Once again successive T-projection chains have their molecular walls oriented up and down so that they interleave to form a double layer in the *a* direction, but this time the walls do not participate in face-face aryl interactions and are all separated by interposed guest molecules. The double layers still stack on top of each other in the sense -a-b-a-b- as shown in Figure 10 (cf. Figure 6). Stabilisation is provided by a centrosymmetric offset *exo*-*exo* aryl face-face attraction (3.62 Å) where a ring nitrogen of one host stacks over a ring carbon of the second (and vice versa), and also an array of weak Br···Br attractions involving two different Br···Br interactions of 3.92 Å.

As before, the top and bottom outer faces of each double layer comprise the alternately subtended wings. Where wings of neighbouring T cross-sectioned chains abut they assemble edge to edge in a manner virtually identical to that present in $(12)_2{\cdot}C_4H_8O$, but due to the increased molecular symmetry this planar contact involves only a single aryl Ar-H···N interaction (3.16 Å) which is repeated infinitely between the wings of adjacent chains (Figure S5, Supporting Information; cf. Figure 7). Similarly there now is only one intermolecular Br···Br (4.26 Å) and one C−*H*···*N* contact (2.73 Å) within the chains.

In structure $(12)_2{\cdot}C_2H_2Cl_4$ the molecular walls subtended inwards from the top of each double layer run parallel to each other throughout the lattice. Those subtended inwards from the bottom of each double layer similarly are parallel to each other, but are out of phase with those from the top, thereby creating rows of parallelepiped-shaped molecular boxes (Figure 11). Each guest molecule positioned between an up and a down molecular wall hence occupies a box whose six sides are aryl wings.

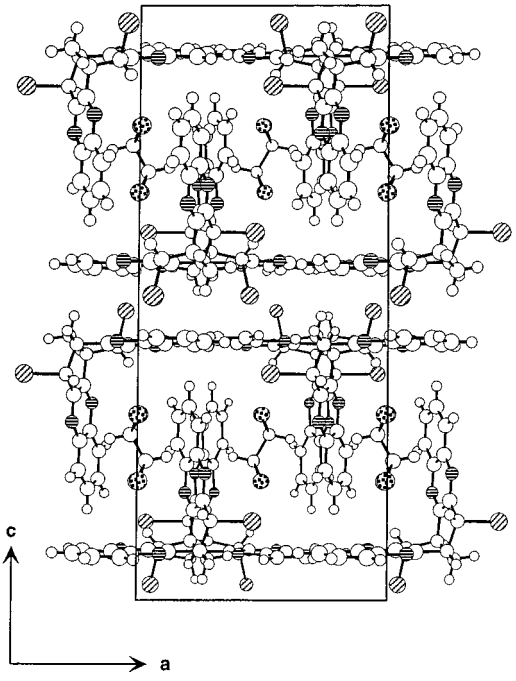

Figure 10. Two double layers, each formed from interleaved T-projection molecular walls, in the structure $(12)_2{\cdot}(CHCl_2{-}CHCl_2)$; in contrast to the structure in Figure 6 the interleaved molecular walls within each double layer do not participate in aryl face-face attractions; instead, tetrachloroethane guest molecules are interposed between all the molecular walls in this lattice

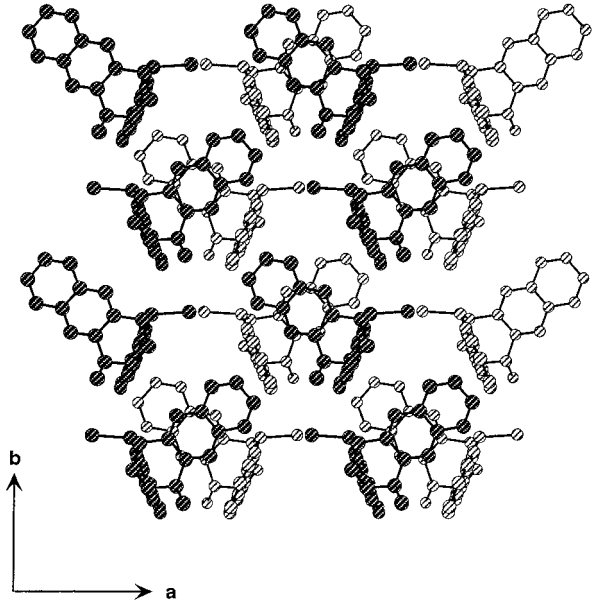

Figure 11. Projection view (cf. Figure 8) in the *ab* plane of a double layer in the structure $(12)_2{\cdot}(CHCl_2{-}CHCl_2)$; while the down-orientated (dark) and up-orientated (light) molecular walls are both individually in phase, they are mutually out of phase; this results in tube constriction and formation of a series of molecular boxes along *b*; each box encloses one guest molecule (omitted here for clarity)

Two of the V-shaped **12** molecules each contribute two *endo*-faces providing four sides, and two further hosts contribute one *exo*-face each to provide the fifth and sixth sides of the box (Figure 12). The outcome resembles a stack of dockside shipping containers except that the array is on a molecular scale and each container contains one 1,1,2,2-tetrachloroethane guest molecule.[29]

Each guest molecule takes part in several types of host-guest interaction. Two of the chlorine atoms have C (host wing) π···Cl (guest) contacts of 3.34, 3.54 and 3.56 Å, while the other two show host-guest Br···Cl interactions of 4.01 Å. Aryl *C*···*H*−CCl_2 contacts of 2.86 and 2.91 Å are also present, and the same hydrogen is also 3.19 Å from a ring nitrogen atom. Finally, the shortest intermolecular host-guest N···C contacts are 3.43 and 3.57 Å. There are no guest-

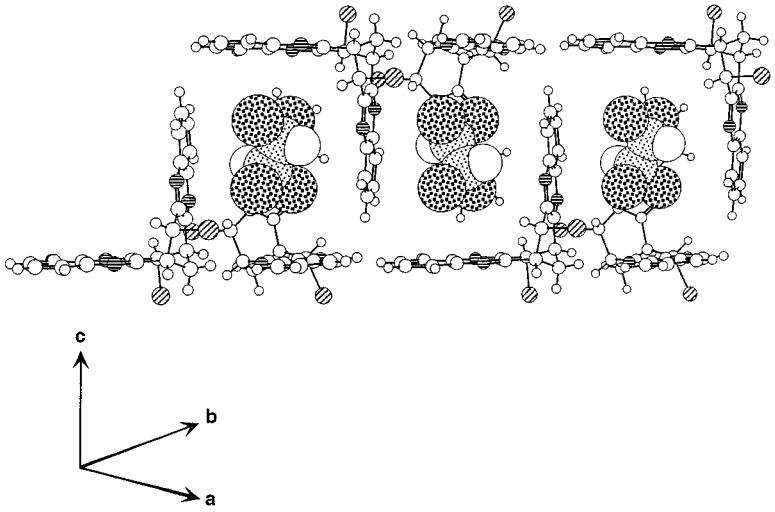

Figure 12. Construction of the molecular boxes in $(\mathbf{12})_2$·$(CHCl_2-CHCl_2)$; four sides of each box are formed from *endo*-faces of two complete host molecules; the remaining two sides are provided by the *exo*-faces of two additional half molecules of **12** (the front examples of which are omitted here for clarity); the 1,1,2,2-tetrachloroethane guest molecules are shown in space-filling representation; guest carbons are lightly, and chlorines heavily, stippled.

guest interactions as each is confined to its own box. Although Toda has provided recent evidence of novel conformations in certain halogenated guest molecules, here the symmetry of the molecular box accommodates the low energy staggered arrangement without further complexity.[30]

Conclusions

While the di(1,8-naphthyridine) derivative **7** proved to be unstable, the diquinoxaline **12** was found to be a versatile new host molecule with a preference for two-carbon polychlorocarbon guests. As anticipated, competition between a number of weak intermolecular interactions led to lattice inclusion compounds of differing structures as the guest was changed. Hence the same host is able to combine with a variety of chlorinated guests of differing size and shape.

This work shows that both single and dimeric C−H···N weak hydrogen bonds (data summarised in Table 2) are important synthons for crystal engineering. In particular they provide the means for the edge-edge assembly of nitrogen heteroaromatic systems, a packing mode not generally available to aromatic hydrocarbons.

It is significant, however, that C−H···N dimers are observed in both diquinoline structures **1** and **2**·$CHCl_3$, and all three diquinoxaline **12** inclusion structures. Three centrosymmetric (aryl C−H···N) and three asymmetric (aryl C−H···N and aliphatic BrC−H···N) weak hydrogen bonded dimers are present in these compounds. Hence dimeric C−H···N interactions, which represent a higher order motif than the single interaction, constitute a robust synthon for use in future crystal engineering experiments.

Experimental Section

^{1}H (300 MHz) and ^{13}C (75 MHz) NMR spectra were recorded with a Bruker ACF300 instrument at 25 °C and are reported as chemical shifts (δ) relative to TMS. The substitution of carbon atoms was determined by the DEPT procedure. − Melting points were determined with a Kofler instrument and are uncorrected. − Mass spectra (electron impact) were recorded on a VG Quattro triple quadrupole instrument by Dr. J. J. Brophy. − IR spectra were recorded on a Perkin−Elmer 298 infrared spectrophotometer. − Elemental analyses were carried out at the University of New South Wales by Dr. H.P. Pham.

6,7,14,15-Tetrahydro-7,15-methanocycloocta[1,2-*b*:5,6-*b*′]di(1′,8′-naphthyridine) (6): 2-Aminonicotinaldehyde[15] (**4**; 2.06 g, 16.9 mmol) and bicyclo[3.3.1]nonane-2,6-dione[16] (**5**; 1.22 g, 8.02 mmol) were dissolved in methanol (4.0 mL) with slight warming. Aqueous NaOH (2.0 M, 2.0 mL) was added dropwise causing darkening of the solution which was stirred at room temp. for 16.5 h. The resulting suspension was filtered and the solid recrystallised ($CHCl_3$/ethyl acetate) to give **6** as fine needles (1.43 g, 55%). M.p. >305 °C. − ^{1}H NMR ($CDCl_3$): δ = 2.53 (t, ^3J = 3.0 Hz, 2 H, H17), 3.43−3.56 (m, 4 H, H7/15), 3.88−3.92 (m, 2 H, H6/14), 7.30 (dd, ^3J = 8.2 and 4.1 Hz, 2 H, H2/10), 7.68 (s, 2 H, H8/16), 7.93 (dd, ^3J = 8.2 Hz, ^4J = 2.1 Hz, 2 H, H1/9), 8.96 (dd, ^3J = 4.1 Hz, ^4J = 2.1 Hz, 2 H, 3/11). − ^{13}C NMR ($CDCl_3$): δ = 28.4 (CH_2), 36.4 (CH), 37.8 (CH_2), 121.5 (CH), 121.6 (C), 129.9 (C), 136.0 (CH), 136.7 (CH), 152.9 (CH), 154.9 (C), 164.8 (C). − IR (nujol mull): $\tilde{\nu}$ = 1610w, 1600w, 1550m, 1375w, 800m, 790w cm^{-1}. − MS; *m*/*z* (%): 325 (22), 324 (100) [M$^+$], 323 (56), 321 (14), 309 (12), 283 (13), 181 (65), 162 (20), 161 (16), 144 (18), 89 (13), 84 (17). − $C_{21}H_{16}N_4$ (324.4): calcd. C 77.75, H 4.97, N 17.28; found C 77.43, H 5.14, N 17.07.

6α,14α-Dibromo-6,7,14,15-tetrahydro-7α,15α-methanocycloocta[1,2-*b*:5,6-*b*′]di(1′,8′-naphthyridine) (7): Compound **6** (203 mg, 0.63 mmol) and *N*-bromosuccinimide (273 mg, 1.53 mmol) were refluxed in $CHCl_3$ for 2 h. The cooled solution was decanted and the yellow residue was shaken with $CHCl_3$ (50.0 mL) and Na_2SO_3 (50.0 mL of a dilute aqueous solution). The $CHCl_3$ portion was dried (Na_2SO_4) and the filtrate evaporated under reduced pressure to give a foam which was chromatographed on silica (7.0 g) using $CHCl_3$/methanol (9:1). The product **7** was obtained as a pale yellow solid (182 mg, 60%) which was pure by ^{1}H NMR spectroscopy. M.p. >300 °C (from CH_2Cl_2/methanol). − ^{1}H NMR ($CDCl_3$): δ = 3.20 (t, ^3J = 3.1 Hz, 2 H, H17), 4.18−4.22 (m, 2 H, H6/14), 5.91

(d, ^3J = 2.0 Hz, 2 H, H7/15), 7.43 (dd, ^3J = 8.2 and 4.1 Hz, 2 H, H2/10), 8.05 (dd, ^3J = 8.2 Hz, ^4J = 2.0 Hz, 2 H, H1/9), 8.07 (s, 2 H, H8/16), 9.09 (dd, ^3J = 4.1 Hz, ^4J = 2.0 Hz, 2 H, H3/11). − ^{13}C NMR ($CDCl_3$): δ = 19.8 (CH_2), 44.5 (CH), 51.0 (CH), 122.3 (C), 122.6 (CH), 130.7 (C), 136.9 (CH), 140.3 (CH), 154.8 (CH), 155.5 (C), 159.0 (C). − IR (nujol mull): ṽ = 1605m, 1545m, 1300w, 1270w, 1240w, 1165w, 1150w, 1140w, 1110w, 1010w, 995w, 940w, 900w, 785s, 775s, 730w, 720m, 670w cm^{-1}. − MS; *m/z*: (%): 484 (1) [M^+ + 2], 482 (^{79}Br + ^{81}Br) (3) [M^+], 480 (1) [M^+ − 2], 403 (22), 401 (21), 323 (24), 322 (43), 321 (100), 320 (26), 161 (37), 160 (22), 86 (17), 84 (27), 49 (40).

1,9-Dibenzyl-6,7,14,15-tetrahydro-7,15-methanocycloocta[1,2-*b*:5,6-*b*′]di(1′,8′-naphthyridine)-1,9-diium Dibromide (8): Compound **6** (59 mg, 0.18 mmol), toluene (5.0 mL), and benzyl bromide (1.0 mL) were refluxed for 15 h. The resulting suspension was filtered, the solid obtained washed with diethyl ether (10.0 mL), and recrystallised from CH_3CN/diethyl ether to give **8** as a red-brown solid (115 mg, 96%). M.p. >300 °C. − ^{1}H NMR [D_6]DMSO: δ = 2.60 (m, 2 H, H17), 3.20−3.26 (m, 2 H), 3.76−3.82 (m, 2 H), 3.94 (br s, 2 H, H6/14), 6.28 and 6.33 (d, ^2J = 13.8 Hz, 2 H, Ar−CH_AH$_B$), 6.36 and 6.41 (d, ^2J = 13.8 Hz, 2 H, Ar−CH$_A$$H_B$), 7.39−7.45 (m, 6 H), 7.60 (m, 4 H), 8.19 (dd, ^3J = 8.2 and 5.6 Hz, 2 H, H2/10), 8.49 (s, 2 H, H8/H16), 9.18 (d, ^3J = 7.7 Hz, 2 H), 9.88 (d, ^3J = 6.2 Hz, 2 H). − ^{13}C NMR [D_6]DMSO: δ = 26.4 (CH_2), 36.3 (CH), 37.4 (CH_2), 57.9 (CH_2), 123.2 (CH), 124.2 (C), 129.2 (CH), 129.3 (CH), 133.9 (C), 134.9 (C), 139.6 (CH), 144.6 (C), 148.5 (CH), 151.0 (CH), 169.5 (C), one Ar−H peak obscured. − IR (paraffin mull) ṽ = 3400br s (OH), 1620m, 1580m, 1500w, 1400m, 1250w, 780m, 760m, 740m cm^{-1}. − $C_{35}H_{30}N_4Br_2$·$3H_2O$ (720.5): calcd. C 58.34, H 5.04, N 7.78; found C 58.94, H 4.82, N 7.30.

6,7,14,15-Tetrahydro-5,8,13,16-tetraoxo-6,14-methanocycloocta[1,2-*b*:5,6-*b*′]diquinoxaline (10); 6,7,14,15-Tetrahydro-6,14-methanocycloocta [1,2-*b*:5,6-*b*′]diquinoxaline (11); and 7α,15α-Dibromo-6,7,14,15-tetrahydro-6α,14α-methanocycloocta[1,2-*b*:5,6-*b*′]diquinoxaline (12): The preparation and characterisation of these compounds has been described in an earlier communication.[29]

Molecular Volume Calculations: These were obtained from crystal structure data using the Insight II program (Version 2.3.6) produced by Biosym Technologies Inc. The van der Waals atomic radii used were those determined by Bondi:[27] C 1.77, H 1.20, N 1.60, O 1.50, Cl 1.75, Br 1.85 Å. The calculated molecular volumes (V_o) were **2** 338, **12** 328, $CHCl_3$ 70, $C_2H_2Cl_4$ 101, and C_4H_8O 81 Å^3 respectively.

The percentage occupancy of a pure crystal is given by 100(Z V_o/V), where V is the unit cell volume, Z is the number of molecules in the unit cell, and V_o is the volume of a single molecule.[20] For the inclusion compounds described here the sums of V_o for hosts and guests, in conjunction with the formula and values of Z and V listed in Table 1, were used. Sample calculation for inclusion compound of **12** and chloroform: Z = 4, V = 2668 Å^3, calcd. V_o for **12** = 328 Å^3, calcd. V_o for $CHCl_3$ = 70 Å^3, sum of V_o values for formula **12**·$(CHCl_3)_2$ = 468 Å^3. ∴ Percentage occupancy = 100 (Z V_o/V) = 100 × 4 × 468/2668 = 70%.

Determination of the Crystal Structures of 12·$(CHCl_3)_2$ and (12)$_2$·C_4H_8O: For **12**·$(CHCl_3)_2$, reflection data were measured with an Enraf−Nonius CAD-4 diffractometer in θ/2θ scan mode using graphite monochromated molybdenum radiation (λ = 0.7107 Å). The crystal was sealed in a Lindeman glass tube to prevent decomposition. Data were not corrected for absorption. The asymmetric unit consisted of one half of the molecule, with a twofold axis parallel to *b*, at x = 1/2, z = 3/4 relating the two halves. The chloroform guest was disordered over two sites, and each was included in the refinement with its occupancy varied, but with the two occupancies constrained to a total of 1. The final values of the occupancies were 0.866(2) and 0.134. A rigid group defined the guest, which had threefold symmetry. A single global C−Cl distance was refined, and its final value was 1.736(3). The position and orientation of each of the two disorder components were refined. The thermal motion of the guest was described by a 15 variable TLX group (where T is the translation tensor, L is the libration tensor and X is the origin of libration).

For (**12**)$_2$·C_4H_8O, reflection data were measured with an Enraf−Nonius CAD-4 diffractometer in θ/2θ scan mode using nickel-filtered copper radiation (λ = 1.5418 Å). Data were corrected for absorption.[31] The THF molecule was disordered and the positions of both components were determined from a difference map. It was difficult to determine the position of the oxygen atom in the guest. Its probable location was assigned by a consideration of host-guest contacts, bearing in mind the difference in overall size of the oxygen and methylene groups. The atoms of the THF were refined individually, with slack constraints imposed to keep all bond lengths approximately equal to 1.45 Å. The occupancies of the guest were refined, with the sum of the occupancies of the two disorder components being maintained at 1. These final values were 0.684(7) and 0.316. The thermal motion of the THF was refined as a 12 parameter TL group. Correct enantiomeric selection was confirmed by the residual, R, which was 0.045 for the structure presented here and 0.047 for the other enantiomer.

For both structures, reflections with $I > 3\sigma(I)$ were considered observed. The structures were determined by direct phasing (MULTAN80)[32] and Fourier methods. Hydrogen atoms for each host were included in calculated positions. Positional parameters for the non-hydrogen atoms of the hosts were refined using full-matrix least-squares using RAELS, a program capable of constrained refinement.[33] Individual anisotropic thermal parameters for each atom were refined for **12**·$(CHCl_3)_2$, while for (**12**)$_2$·C_4H_8O the thermal motion of each independent host molecule was refined as a 15 parameter TLX group. The reflection weights used were $1/\sigma^2(F_o)$, with $\sigma(F_o)$ being derived from $\sigma(I_o) = [s^2(I_o) + (0.04I_o)^2]^{1/2}$. The weighted residual was defined as $R_w = (\Sigma w\Delta F^2/\Sigma wF_o^2)^{1/2}$. Atomic scattering factors and anomalous dispersion parameters were from International Tables for X-ray Crystallography.[34]

Supplementary crystallographic data (excluding structure factors) for the structures **12**·$(CHCl_3)_2$ and (**12**)$_2$·C_4H_8O have been deposited with the Cambridge Crystallographic Data Centre as supplementary publication nos. CCDC-144862 and 144863, respectively. Copies of the data can be obtained free of charge on application to CCDC, 12 Union Road, Cambridge CB2 1EZ U.K. [Fax: (internat.) +44-1223/336-033; E-mail: deposit@ccdc.cam.ac.uk]. Preliminary details of structure (**12**)$_2$·$C_2H_2Cl_4$ are published[29] and full crystallographic data are available through CSD refcode TAZMIQ.

Five additional figures, as mentioned in the text, are available as Electronic Supporting Information.

Acknowledgments

We thank the Australian Research Council for financial support of this work.

[1] *Inclusion Compounds* (Eds.: J. L. Atwood, J. E. D. Davies, D. D. MacNicol), Vol. 1−3, Academic Press, London, **1984**; Vol. 4−5, Oxford University Press, Oxford, **1991**.

[2] *Comprehensive Supramolecular Chemistry*, Vol. 6, *Solid State Supramolecular Chemistry: Crystal Engineering* (Eds.: D. D. MacNicol, F. Toda, R. Bishop), Pergamon, Oxford, **1996**.

[3] R. Bishop, *Chem. Soc. Rev.* **1996**, *25*, 311−319.

[4] [4a] G. R. Desiraju, *Crystal Engineering: The Design of Molecular Solids*, Elsevier, Amsterdam, **1989**. − [4b] G. R. Desiraju, C. V. K. Sharma, in *The Crystal as a Supramolecular Entity* (Ed.: G. R. Desiraju), Wiley, New York, **1996**, Ch. 2, pp. 31−61.

[5] G. R. Desiraju, *Angew. Chem. Int. Ed. Engl.* **1995**, *34*, 2311−2327.

[6] [6a] R. Taylor, O. Kennard, *J. Am. Chem. Soc.* **1982**, *104*, 5063−5070. − [6b] Z. Berkovitch-Yellin, L. Leiserowitz, *Acta Crystallogr., Sect. B* **1984**, *40*, 159−165. − [6c] D. S. Reddy, B. S. Goud, K. Panneerselvam, G. R. Desiraju, *J. Chem. Soc., Chem. Commun.* **1993**, 663−664. − [6d] D. S. Reddy, D. C. Craig, G. R. Desiraju, *J. Chem. Soc., Chem. Commun.* **1994**, 1457−1458. − [6e] M. Mascal, J. L. Richardson, A. J. Blake, W.-S. Liu, *Tetrahedron Lett.* **1996**, *37*, 3505−3506. − [6f] R. Thaimattam, D. S. Reddy, F. Xue, T. C. W. Mak, G. R. Desiraju, *J. Chem. Soc., Perkin Trans. 2* **1998**, 1783−1789. − [6g] C. Foces-Foces, N. Jagerovich, J. Elguero, *Acta Crystallogr., Sect. C* **2000**, *56*, 215−218.

[7] For discussion and a comprehensive review of C−H···N and other weak hydrogen bonding motifs, see: G. R. Desiraju, T. Steiner, *The Weak Hydrogen Bond in Structural Chemistry and Biology*, Oxford Science Publications, Oxford, **1999**; in particular Ch. 2, pp. 29−121 and Ch. 4, pp. 293−342.

[8] R. S. Rowland, R. Taylor, *J. Phys. Chem.* **1996**, *100*, 7384−7391.

[9] A. Gavezzotti, *Cryst. Rev.* **1998**, *7*, 5−121.

[10] C. E. Marjo, M. L. Scudder, D. C. Craig, R. Bishop, *J. Chem. Soc., Perkin Trans. 2* **1997**, 2099−2104.

[11] [11a] V. R. Pedireddi, W. Jones, A. P. Chorlton, R. Docherty, *Chem. Commun.* **1996**, 997−998. − [11b] F. A. Cotton, L. M. Daniels, G. T. Jordan, IV, C. A. Murillo, *Chem. Commun.* **1997**, 1673−1674. − [11c] M. Mascal, *Chem. Commun.* **1998**, 303−304.

[12] [12a] C. E. Marjo, R. Bishop, D. C. Craig, A. O′Brien, M. L. Scudder, *J. Chem. Soc., Chem. Commun.* **1994**, 2513−2514. − [12b] R. Bishop, C. E. Marjo, M. L. Scudder, *Mol. Cryst. Liq. Cryst.* **1998**, *313*, 75−83.

[13] [13a] A. Clearfield, M. J. Sims, P. Singh, *Acta Crystallogr., Sect. B* **1972**, *28*, 350−355. − [13b] P. Dapporto, C. A. Ghilardi, C. Mealli, A. Orlandini, S. Pacinotti, *Acta Crystallogr., Sect. C* **1984**, *40*, 891−894.

[14] C.-C. Cheng, S.-J. Yang, *Org. React.* **1982**, *28*, 37−201.

[15] T. G. Majewicz, P. Caluwe, *J. Org. Chem.* **1974**, *39*, 720−721.

[16] J. P. Schaefer, L. M. Honig, *J. Org. Chem.* **1968**, *33*, 2655−2659.

[17] F. H. Allen, J. E. Davies, J. J. Galloy, O. Johnson, O. Kennard, C. F. Macrae, E. M. Mitchell, G. F. Mitchell, J. M. Smith, D. G. Watson, *J. Chem. Inf. Comput. Sci.* **1991**, *31*, 187−204.

[18] [18a] C. H. Issidorides, M. J. Haddadin, *J. Org. Chem.* **1966**, *31*, 4067−4068. − [18b] M. J. Haddadin, M. U. Taha, A. A. Jarrar, C. H. Issidorides, *Tetrahedron* **1976**, *32*, 719−724.

[19] F. B. Mallory, *Org. Synth.* **1963**, *Collect. Vol. 4*, 74−78.

[20] [20a] A. I. Kitaigorodsky, *Acta Crystallogr.* **1965**, *18*, 585−590. − [20b] A. I. Kitaigorodsky, *Molecular Crystals and Molecules*, Academic Press, New York, **1973**.

[21] A. I. Kitaigorodsky, *Mixed Crystals*, Springer-Verlag, Berlin, **1984**, pp. 283−318.

[22] [22a] O. Hassel, C. Rømming, *Quart. Rev.* **1962**, *16*, 1−18.[22b] H. A. Bent, *Chem. Rev.* **1968**, *68*, 587−648. − [22c] D. S. Reddy, D. C. Craig, G. R. Desiraju, *J. Chem. Soc., Chem. Commun.* **1993**, 1737−1739. − [22d] S. C. Blackstock, J. P. Lorand, J. K. Kochi, *J. Org. Chem.* **1987**, *52*, 1451−1460. − [22e] S. C. Blackstock, J. K. Kochi, *J. Am. Chem. Soc.* **1987** *109*, 2484−2496. − [22f]J.-M. Dumas, H. Peurichard, M. Gomel, *J. Chem. Res. (S)* **1978**, 54−55.

[23] D. S. Reddy, K. Panneerselvam, T. Pilati, G. R. Desiraju, *J. Chem. Soc., Chem. Commun.* **1993**, 661−662.

[24] K. Xu, D. M. Ho, R. A. Pascal, Jr., *J. Am. Chem. Soc.* **1994**, *116*, 105−110.

[25] [25a] J. A. R. P. Sarma, G. R. Desiraju, *Acc. Chem. Res.* **1986**, *19*, 222−228. − [25b] H. Krupitsky, Z. Stein, I. Goldberg, *J. Incl. Phenom.* **1995**, *20*, 211−232.

[26] [26a] M. Bremer, P. S. Gregory, P. v. R. Schleyer, *J. Org. Chem.* **1989**, *54*, 3796−3799. − [26b] V. R. Pedireddi, D. S. Reddy, B. S. Goud, D. C. Craig, A. D. Rae, G. R. Desiraju, *J. Chem. Soc., Perkin Trans. 2* **1994**, 2353−2360.

[27] A. Bondi, *J. Phys. Chem.* **1964**, *68*, 441−451.

[28] J. Jacques, A. Collet, S. H. Wilen, *Enantiomers, Racemates and Resolutions*, Wiley, New York, **1981**, Ch. 2.2, pp. 43−88.

[29] A preliminary communication of this structure has been published: C. E. Marjo, R. Bishop, D. C. Craig, M. L. Scudder, *Aust. J. Chem.* **1996**, *49*, 337−342.

[30] F. Toda, K. Tanaka, R. Kuroda, *Chem. Commun.* **1997**, 1227−1228.

[31] J. de Meulenaer, H. Tompa, *Acta Crystallogr.* **1965**, *19*, 1014−1018.

[32] P. Main, S. J. Fiske, S. E. Hull, L. Lessinger, G. Germain, J.-P. Declercq, M. M. Woolfson, *MULTAN80: A System of Computer Programs for the Automatic Solution of Crystal Structures from X-ray Diffraction Data*, Universities of York, England, and Louvain, Belgium, **1980**.

[33] A. D. Rae, *RAELS. A Comprehensive Constrained Least Squares Refinement Program*, University of New South Wales, **1996**.

[34] *International Tables for X-ray Crystallography* (Eds.: J. A. Ibers, W. C. Hamilton), Vol. 4, Kynoch Press, Birmingham, **1974**.

Received June 22, 2000
[O00315]